Supplementary data

Tubulin-folding cofactor E deficiency promotes vascular dysfunction by increased endoplasmic reticulum stress.

Panagiotis Efentakis[1,2], Michael Molitor[1,2,3], Sabine Kossmann[1,2], Magdalena L. Bochenek[1,2,3], Johannes Wild[1,2], Jeremy Lagrange[1,2], Stefanie Finger[2], Rebecca Jung[2], Susanne Karbach[1,2,3], Katrin Schäfer[1,3], Andreas Schulz[4], Philipp Wild[2,3,4], Thomas Münzel[1,2,3 #], Philip Wenzel[1,2,3 # *]

[1] Department of Cardiology, University Medical Center Mainz

[2] Center for Thrombosis and Hemostasis, University Medical Center Mainz

[3] German Center for Cardiovascular Research (DZHK) - Partner site Rhine-Main

[4] Department of Cardiology - Preventive Cardiology and Medical Prevention, University Medical Center Mainz

[#] equal contribution

***Address for correspondence:** Philip Wenzel, Department of Cardiology and Center for Thrombosis and Hemostasis, University Medical Center Mainz, Langenbeckstraße 1, 55131 Mainz, Germany, Phone: +49 6131 17 7695, E-Mail: wenzelp@uni-mainz.de

Supplementary Methods

Genome-wide association study (GWAS)

SNP information was gained from the genome data available from the Gutenberg Health Study (GHS) as previously described [1]. Genotyping was conducted on Affymetrix Genome-Wide Human SNP 6.0 arrays (Affymetrix, Santa Clara, CA) according to the manufacturer´s recommendations for a population sample of 5,000 individuals. After a quality control review, genetic data were available for analysis in 4,175 individuals. Before genotype imputation, SNPs with a significant ($P < 10^4$) deviation from the Hardy-Weinberg equilibrium with minor allele frequency <1% or having a genotyping call rate <98% were excluded. Correlation analysis by linear regression was performed in order to identify SNPs that were associated with flow mediated dilation (FMD).

The Genotype-Tissue Expression (GTEx) Project was supported by the Common Fund of the Office of the Director of the National Institutes of Health, and by NCI, NHGRI, NHLBI, NIDA, NIMH, and NINDS. The data used for the analyses described in this manuscript were obtained from the GTEx Portal and dbGaP accession number phs000424.vN.pN on June 2019.

Animals

Three different strains of cell-specific, conditional TBCE knockout mice were generated by serial crossings. $TBCE^{tm1c}$ mice were first generated according to EUCOMM® instructions [2, 3] in a “flippase-first” approach to generate $TBCE^{tm2c}$ and then crossed with $Cre^{+/-}$ mice to create the conditional knockout mice $Cre^{+/-}TBCE^{fl/fl}$ (C57BL/6J background). The Cre transgene was kept only in the male breeders, while female breeders were Cre-negative ($Cre^{-/-}$) in order to avoid germline deletion of the gene [4]. $LysMCre^{+/-}TBCE^{fl/fl}$ mice were generated as myeloid cell specific deficiency of TBCE [5], $Tie2\text{-}ERT2Cre^{+/-}TBCE^{fl/fl}$ mice as a conditional knockdown model in endothelial cells [6], and $SMMHC\text{-}ERT2Cre^{+/-}TBCE^{fl/fl}$ as a conditional knockdown model in smooth muscle cells [7]. For all the above-mentioned strains, age-matched $Cre^{+/-}TBCE^{wt/wt}$ littermates were used as controls in all experiments. $Tie2\text{-}ERT2Cre^{+/-}TBCE^{fl/fl}$ mice and their respective control were fed tamoxifen diet (Envigo®, Horst, Netherlands) for the activation of the Cre gene for 8 weeks starting at the age of 3-4 weeks, while $SMMHC\text{-}ERT2Cre^{+/-}TBCE^{fl/fl}$ mice were fed with tamoxifen-containing rodent chow (Envigo®, Horst, Netherlands) for 6 weeks starting at an age of 5-6 weeks. A total of 60 $LysMCre^{+/-}TBCE^{fl/fl}$, 80 $Tie2\text{-}ERT2Cre^{+/-}TBCE^{fl/fl}$ and 140 $SMMHC\text{-}ERT2Cre^{+/-}TBCE^{fl/fl}$ mice were used in the experiments. Mice were housed under SPF conditions with a maximum of 5 animals per cage. All animals were inbred and received proper care in compliance with the Guide for the Care and Use of Laboratory Animals published by the US National Institutes of Health (NIH Publication No. 85-23, revised 1985) and were approved by the Ethical Committee of the Prefecture of Rheinland-Pfalz (G17-1-031). All animal experiments were performed in line with ARRIVE guidelines [8].

All animals were 12-14 weeks of age at the time of experimentation. Before organ harvest, animals were euthanized by an overdose of isoflurane, followed by cervical dislocation. To minimize the effect of subjective bias, animals were randomly assigned to the groups in each experimental design. Researchers in the final experimentation (organ harvest) were blinded to the strains. The breeding strategy, genotyping and workflow are described in **Figure S2**. For the in vivo experiments sample size was calculated using G*POWER 3.1.9.2 software (Power 0.8, α error prob. 0.05, F-Test, ANOVA: Fixed effects, omnibus, one-way). Primary endpoints were preselected prior to the initiation of the in vivo experiments. Animals that did not meet the wellbeing criteria regarding the 3Rs were excluded from the experiments, while no outliers were removed from the experiments

Genotyping: For the generation of the tm1c mice, the genotype of the animals was identified by RCR analysis of genomic DNA gained from tail samples of the mice using Mouse Direct PCR Kit according to the manufacturer's instructions (B45012, Biomake.com). For *tbce* a band at 500bp corresponds to the "pseudo-wt" or floxed mice, a double band at 300-500 bp to the heterozygote mice, while a single band at 400 bp indicates a wild-type animal. For *tm1c*, the presence of a band at 300 bp indicate the presence of the construct which is perquisite for the generation of the floxed mice. In the same mice an absence of a band at 300 bp for the 5FRT and FLP is necessary, indicating the removal of the 5FRT and FLP constructs from the genome (**Figure S2** upper panel).

For the LysMCre$^{+/-}$TBCE^{tm2c} mice, a band at 300-400 bps using the LysM wt PCR primers indicates the absence of Cre in at least one of the two strands, while a band at 700-900 bps using the LysM tg PCR primers indicate the presence of Cre in at least one of the two strands. The identification of TBCE$^{wt/wt}$ and TBCE$^{fl/fl}$ mice was conducted as previously described, while for the successful cleavage of the gene the tm1d PCR was conducted and confirmed with a PCR band between 100-200 bps (**Figure S2** second row panel).

For Tie2-ERT2-Cre$^{+/-}$TBCE^{tm2c} mice, the presence of Cre was confirmed with the respective Tie2-ERT2-Cre PCR primers, where the presence of the gene was confirmed with a band at 400 bps. The heterozygote genotype of the Tie2-ERT2-Cre$^{+/-}$TBCE^{tm2c} mice was secured by heterozygote breeding of the mice concerning the Cre, while TBCE and tm1c PCRs where conducted as previously described (**Figure S2** third row panel).

For SMMHC-ERT2-Cre$^{+/-}$TBCE^{tm2c} mice the presence of Cre was confirmed with the respective SMMHC-ERT2-Cre PCR primers. A single band at 200 bps represented the Cre$^{-/-}$ mice, a double band at 300-200bps represented the heterozygote Cre$^{+/-}$ mice. Genotyping was performed for all strains according to EUCOMM® instructions [2, 3]. According to EUCOMM terminology, tm2c symbolizes the transgenic mice with the floxed gene.

Serum postprandial blood glucose, triglycerides and total cholesterol measurements: For serum postprandial blood glucose, triglycerides and total cholesterol, samples were measured by the Central Laboratory of Johannes Gutenberg Medical Center, in Mainz, using an automated analyzer Alinity ci-series (Abbott Core Laboratory - Abbott Diagnostics). Results were expressed as mg/dl.

Angiotensin II infusion: In selected experiments, mice were infused with Angiotensin II (AngII) (1 mg/kg/d for 7 days) via subcutaneously implanted osmotic mini-pumps (model 1007D, ALZET; dorsal implantation between the scapulae); sham-operated mice, implanted with osmotic mini-pumps fill with solvent (saline) served as controls [9]. For pump implantation, mice initially administered buprenorphine (0.075 mg/kg i.p.) 30' prior to the surgery and were subsequently anesthetized with a mixture of medetomidine (500µg/kg), fentanyl (50µg/kg) and midazolam (5mg/kg). As an antidote to the anesthesia, atipamezol (2.5mg/kg) and flumazenil (0.5 µg/kg) were administered to the mice, which rapidly gained consciousness [10]. The very well established s.c. administration of AngII as a common hypertensive stimulus was selected in the *in vivo* studies to model vascular and cardiac dysfunction, which is representative of the hypertensive phenotype in clinical practice. The one-week administration of AngII at the selected dose was previously shown to induce hypertension in mice [10].

Vascular Relaxation and Constriction studies: To assess vasodilator potential of isolated aortic segments (3 mm), they were mounted to force transducers in organ chambers to test their response to acetylcholine (ACh) and nitroglycerine (Glycerol trinitrate, GTN). The aortic rings were pre-constricted with prostaglandin F2 α (PGF2α, 3 nM), a VSMC-dependent constrictor [11]) to reach 50 to 80% of the tone induced by KCl. Concentration-relaxation curves were recorded in response to the endothelium-dependent vasodilators ACh (1 nM to 3 mM) and GTN (1 nM to 30 mM) [9].

Ultrasound evaluation of cardiac, aortic and carotid function: Ultrasound evaluation was performed in anesthesia using a VEVO3100 high-resolution imaging system (VisualSonics®, FujiFilm, Toronto, CA). Mice were anesthetized with isoflurane (1.2 to 1.5 Vol %). Left ventricular function was analyzed in sham and Ang-II treated mice. Equipped with a 38 MHz (MZ400) linear array transducer, images were acquired at a frame rate consistently above 200 frames. ECG and breathing rate were monitored, body temperature was kept at 37 °C using a heating system within the handling platform. In addition, an infrared warming lamp was used when required. Brightness (B)-mode movies and Motion (M)-mode of the parasternal long axis (PLAX) and parasternal short axis (SAX, mid-ventricular) were acquired. Post-acquisition analysis was performed with the VevoLab Software (VisualSonics®, FujiFilm, Toronto, CA).

Left ventricular ejection fraction (LVEF)and Left ventricular end-diastolic volume (LVEDV) were calculated from B-Mode images in PLAX [10]. For aortic diameters, ascending and transverse aortic sections were measured according to the literature [12].

Histology: Aortic sections (3 mm) were fixed in 4% zinc formaline for 24 h and subsequently sliced in 5 µm-thick cross-sections. Slides were de-paraffinized in xylene and rehydrated in serial ethanol concentrations. Sections were stained with hematoxylin and eosin or Sirius Red to histologically evaluate vessel wall thickness and collagen deposition, respectively [13]. For the assessment of the wall thickness, aortic media thickness (internal elastic lamina to the adventitial border [14]) was taken under consideration, as observed by brightfield microscopy after hematoxylin eosin staining. Collagen thickness was measured under polarized microscopy so that the red signal of the staining would be sharper and well defined. At least 10 individual areas of the pictures were measured among the vascular wall and results were averaged per animal into one n value. Collagen thickness was expressed as a ratio to the media thickness [15], namely as Collagen to media thickness. Media and collagen thickness were measured using ImageJ software and by taking under consideration the scale and magnification of the images. For immunofluorescence (IF) experiments, aortic sections were frozen in OCT medium (Tissue-Tek® O.C.T.™ Compound, Fisher Scientific) and sliced in 3 µm-thick cryosections.

Blood pressure assessment: For the measurement of arterial diastolic and systolic blood pressure, mice underwent a non-invasive tail-cuff blood pressure assessment using the Coda Monitor System (Kent Scientific) [9].

Quantitative Real-Time PCR: For isolation of RNA, snap-frozen mouse aortas were pulverized and extracted using the standardized Trizol protocol. RT-PCR was performed with the CFX96 Real-Time PCR Detection System (Bio-Rad, Munich, Germany). Isolated RNA was reverse-transcribed to cDNA using high-capacity cDNA reverse transcription kit (#4368813, Thermo Fisher Scientific). TaqMan Gene Expression Assays were used as the probe and primer sets (Applied Biosystems, Foster City, CA) for Actb (Mm00607939_s1), Ccl2 (Mm00441242_m1), Cd68 (Mm03047340_m1), Cybb (Mm00432775_m1), Il6 (Mm00446190_m1), Il1β (Mm00434228_m1), Gapdh (Mm99999915_g1), Lcn2 (Mm01324470_m1), Ly6c1+2 (Mm03009946_m1), Mmp2 (Mm00439498_m1), Mmp9 (Mm00442991_m1), Nos2 (Mm00440485_m1), Nos3 (Mm00435204_m1), Nox4 (Mm00627696_m1), Tgfβ (Mm01298616_m1), Tnfa (Mm00443260_g1), Vcam-1 (Mm00449197_m1) and Vegf (Mm01281449_m1). Primers for Tbce (F: GGAGGCTCTTTTGTTCGTCC, R: TCGAGCACATAGCGCTTCTT), Tub1A (F:

TGTATGTGGCAATGTGTGCT, R: TGAAATGGGCAGCTTGGGTC), Cdh5 (F: GCTGGAGATTCACGAGCAGT, R: CCACCGCGCACAGAATTAAG), Gapdh (F: TACCCCCAATGTGTCCGTCGTC R: CCTTCAGTGGGCCCTCAGATGC) were analyzed by the standardized SYBR®Green method (Applied Biosystems, Thermo Fisher) according to the manufacturer's instructions [9].

For the human *Tbce* mRNA expression analysis in Figure 1B concerning the peripheral blood mononuclear cells from the 5000 idividuals the following primers were used TBCE: Hs001625_m1 and TBP: Hs00427620_m1 (TaqMan™; Applied Biosystems) as described above.

For RT-PCR analysis of the LysMCre$^{+/-}$TBCE^{tm2c} peripheral blood mononuclear cells (PBMCs), spleen and aorta the following primers were used: Eukaryotic translation initiation factor 2 alpha kinase 3 (*eif2ak3*; F: GCATCGTAGCCACGACCTTC, R: TCAGACTCCTTCCGCCTG), musculus endoplasmic reticulum (ER) to nucleus signaling 1 (*ern1*; F: GCAGCAGACTTTGTCATCGG, R: GGTGATGGTGTATTCTGTCCGT), calnexin (*canx,* F: ACCGGAAGCCTGAAGATTGG, R: TGGGATCTTAGAAGGGGCGT), protein disulfide isomerase associated 3 (*pdia3*; F: AGCAGGACCAGCTTCAGTTC, R: AAAAACCCACCACTGAGGCA), DNA-damage inducible transcript 3 (Ddit3; F: CCTGAGGAGAGAGTGTTCCAG, R: GACCAGGTTCTGCTTTCAGGT), NLR family, pyrin domain containing 3 (*nlrp3*; F: CCTTGGACCAGGTTCAGTGT, R: CAGCAGTTCACCAGTCTGGAA), NLR family, pyrin domain containing 1A (*nlrp1a*, F: CCAATGGCCATCTGAGTTTCC, R: GGGAAGGCCAAAAGGGATCA). RT-PCR analysis was performed by the standardized SYBR®Green method (Applied Biosystems, Thermo Fisher) according to the manufacturer's instructions [9]

Primary Pulmonary Endothelial Cell isolation: Primary mouse endothelial cells were isolated from Tie2-ERT2Cre$^{+/-}$TBCE$^{wt/wt}$ and TBCE$^{fl/fl}$ mouse lungs using magnetic cell sorting (MACS) following CD45^{-}/CD31^{+} (Miltenyi Biotec) selection as described [16]. Mice were sacrificed by cervical dislocation under deep anesthesia with isoflurane. Primary endothelial cells were cultivated in Endothelial Cell Growth Medium 2 (PromoCell) according to the manufacturer's instructions.

Primary Vascular Smooth Muscle Cell isolation: Mouse aortas were aseptically prepared and perivascular adipose tissue was removed. Aortas were cut in 1 mm rings and digested for 5-6 h in Dulbecco's Modified Eagle's Medium [DMEM, 10% Fetal Bovine Serum (FBS)] supplemented with collagenase type II (1.42 mg/mL, # S8N10850, Worthington). The digestion mixture was plated on a 6-well plate for 5 days until VSMCs were confluent, and cells were then subsequently divided according to the experiments [17]. Mice were sacrificed by

cervical dislocation under deep anesthesia with isoflurane. Vascular Smooth Muscle Cells were cultivated in Smooth Muscle Cell Growth Medium 2 (PromoCell) according to the manufacturer's instructions.

siRNA transfection of Human Aortic Smooth Muscle cells: Primary Human Aortic Smooth Muscle Cells (HAoSMCs, PromoCell) were seeded in 75 mL flasks in optimal Smooth muscle cell growth medium (Smooth muscle cell growth medium kit 2, PromoCell) until they reached confluency. Cells were seeded in 96-well plates for the investigation of proliferation rate and in 24-well plates for staining, at a cell number of 6 x 10^3 and 4 x 10^4 cells per well, respectively. Transfection with TBCE siRNA (10 µM, EHU021091, Sigma Aldrich) or siRNA Fluorescent Universal Negative Control (NgCTL, 10 µM, SIC004, Sigma Aldrich) was performed by the siPORT™ NeoFX™ Transfection Agent (AM4510, Thermo Fisher Scientific) for 24 h according to the manufacturer's instructions.

MTT proliferation assay: VSMCs were plated at a density of 6x10^3 cells/well in 96-well plates. Cells were allowed to adhere and treated with AngII (100 nM) for 24 h in the respective groups, while controls were incubated in DMEM as vehicle. Subsequently, cells were incubated with MTT solution [3-(4,5-dimethylthiazol-2-yl)-2,5-diphenyl tetrazolium bromide] (#M-5655, Sigma Aldrich) at a final concentration of 0.5 mg/mL for 4 h at 37 °C. The medium was then aspirated and the formed formazan debris solubilized in dimethylsulfoxide (DMSO). Absorbance was measured at 570 nm (reference wavelength 690 nm) in a microplate spectrophotometer (Tecan Spark, Tecan Inc.).

Western blot analysis: Aortic tissue powder or cells were extracted with lysis buffer (1% Triton X-100, 20 mM Tris pH 7.4-7.6, 150 mM NaCl, 50 mM NaF, 1 mM EDTA,1 mM EGTA, 1 mM Glycerolphosphatase, 1% SDS, 100 mM phenylmethylsulfonyl fluoride, and 0.1% protease phosphatase inhibitor cocktail). After centrifugation (11,000 x g, 15 min, 4 °C), supernatants were used for protein analysis, as previously described [18]. The following primary antibodies were used: NLRP3 (D4D8T) (Rabbit mAb, #15101), NLRC4 (D5Y8E) (Rabbit mAb, #12421), Cleaved Caspase-1 (Asp297) (D57A2) (Rabbit mAb, #4199), β-tubulin (Rabbit mAb , #2146), Calnexin (C5C9) (Rabbit mAb, #2679), IRE1α (14C10) (Rabbit mAb, #3294), PDI (C81H6) (Rabbit mAb, #3501), CHOP (L63F7) (Mouse mAb, #2895), PERK (D11A8) (Rabbit mAb, #5683), Bip (C50B12) (Rabbit mAb, #3177), Beclin-1 (D40C5) (Rabbit mAb, #3495), LC3B (D11) (Rabbit mAb, #3868), pmTOR (Ser2448) (D9C2) (Rabbit mAb #5536), mTOR (7C10) (Rabbit mAb, #2983), p-Raptor (Ser792) (Rabbit mAb #2083), Raptor (24C12) (Rabbit mAb #2280), GAPDH (D16H11) (Rabbit mAb, #5174) (Cell Signaling Technology), TBCE (Rabbit pAb, #NBP1-81713, Novus Biologicals) and eNOS (Mouse mAb, # 610297 BD

Biosciences). PVDF membranes were then incubated with secondary antibodies for 2 h at room temperature [goat anti-mouse (#7076) and goat anti-rabbit HRP (#7074); Cell Signaling Technology, Beverly, MA, USA] and developed using the GE Healthcare ECL Western Blotting Detection Reagents (Thermo Scientific Technologies). Relative densitometry was determined using a computerized software package (NIH, USA), and relative ratios were used for statistical analysis [18].

Murine and human Peripheral Blood Mononuclear Cells Isolation: For peripheral blood mononuclear cells (PBMCs) isolation, whole blood was collected in EDTA-tubes and subsequently cells were isolated using the Lymphoprep™ solution (STEMCELL Technologies) according to the manufacturer's instruction.

Renal tissue analysis and confocal imaging: For glomeruli microcirculation imaging, kidney samples from SMMHC-ERT2Cre$^{+/-}$-TBCE^{tm2c} and Tie2-ERT2-Cre$^{+/-}$-TBCE^{tm2c} mice were embedded in OCT medium. Subsequently cryosections (10 µm) were generated in a cryotome and slides were stained against α-smooth muscle actin (αSMA), TBCE and DAPI. Glomeruli structures were identified under brightfield observation of the slide and also as areas of dense DAPI signal which is not evident in renal tubules. At least 6 images per slide were generated and data were averaged per sample and presented as one n value.

Confocal microscopy: Cells were washed once with PBS and fixed in 4% PFA. Afterwards cells were permeabilized with 0.1% TritonX in PBS, and non-specific binding of the antibodies was blocked by incubation for 1 h in 1% BSA-0.01% Tween-80 in PBS. Cryosections were fixed with 4% PFA, permeabilized with 0.25% TritonX in PBS and blocked with 3% BSA-0.01% Tween-80 in PBS. Subsequently, samples were incubated with TBCE (Rabbit pAb, #NBP1-81713, Novus Biologicals), α-tubulin (Mouse mAb, # A11126 Thermo Fisher Scientific) calnexin (C5C9) (Rabbit mAb, #2679, Cell Signaling Technology), CD31 (Rat mAb, #DIA-310, Dianova), α-Smooth Muscle actin/α-SMa (Mouse mAb, # ab7817, Abcam). Primary antibodies were incubated overnight, washed off with PBS and subsequently anti-rabbit/Alexa-Fluor 647 (Donkey, # ab150079, Abcam), anti-mouse/Alexa-Fluor 647 (Donkey, #ab150107, Abcam) and anti-rat/Alexa-Fluor 594 (Donkey, #ab150160, Abcam) conjugated secondary antibodies were added. After washing twice in PBS, specimens were treated with anti-fade mount medium containing DAPI (P36962, Thermo Fisher Scientific) and visualized in a confocal laser-scanning microscope (Leica SP8 confocal microscope, 63×, oil immersion objective). Z stacks were obtained and 3D images were generated using Fiji-Image J software2 [18]. At least 6 different areas were imaged per slide and results were averaged into one n value. Images to be quantified were acquired and exported in 12-bit grayscale format and aberrations were

corrected using Fiji-Image J software. Relative quantitation was performed in images with even illumination across the field. Control slides with positive signal for each fluorophore were used for each staining to apply corrections. Constant acquisition settings were maintained among the samples with the same staining. The lowest laser power that provided a sufficient signal-to-noise ratio was used in every imaging. Fluorophore intensity was represented as integrated fluorescence density in the figures and was normalized to the DAPI signal of the respective image. Acquisition of the images were performed according to confocal microscopy guidelines [19].

Flow cytometric analysis: Aortas were isolated from mice and prepared free from perivascular adipose tissue. Aortas were shredded mechanically with razor blades and consecutively digested using a Liberase TM mixture (1mg/ml RPMI medium, Roche) for 30 minutes at 37 °C. Cell solutions were passed over 70 µm nylon cell strainers and flushed with PBS/FCS (2%). Aortic cells were incubated with anti-CD-16/CD-32 to prevent unspecific antibody binding. Afterward, cells were washed and incubated with viability dye and fluorophore-labeled antibodies against surface epitopes of cells: viability dye, eFluor 506, eBioscience; anti-CD45.2 APC-Cy7, eBioscience; CD31, PE, Biolegend; CD11b, PE-Cy7, eBioscience; Ly6G, FITC, Biolegend; Ly6C, Pacific Blue, BD Bioscience; F4/80, APC, Biolegend; CD19 PerCP, Biolegend; CD90.2, APC-Cy7, eBioscience. The stained cell solutions were acquired using a FACS Canto II flow cytometer (BD Bioscience) and analyzed using FlowJo Software (BD Bioscience).

TUDCA in vivo and in vitro experiments: In vivo: SMMHC-ERT2Cre$^{+/-}$-TBCE^{tm2c} mice were fed *ad libitum* with tamoxifen food, as stated above for 6 weeks (**Figure S2**). During the 4th week of their tamoxifen diet, Tauroursodeoxycholic acid (TUDCA; #14605-22-2, Cayman Chemical, USA) was administered daily via oral gavage at a dose of 300 mg/kg body weight [20], dissolved in normal saline (250 µL/mouse) for 10 days. Control mice received an equal volume of normal saline. At the end of the 10-day treatment, animals were sacrificed by isofluorane overdose and whole blood as well as aortic samples were obtained. In vitro: Primary VSMCs from SMMHC-ERT2Cre$^{+/-}$-TBCE$^{fl/fl}$ mice were isolated [17] and seeded at a plating number of 6 x 10^3 cells per well in a 96 well plate. Cells were allowed to attach and then treated either with starvation medium (DMEM, 1% FCS, 1% PenStrep) or with TUDCA (dissolved in starvation medium) at a concentration of 1 mM for 24 h [21]. Subsequently, cellular viability was assessed using the MTT assay.

Statistical Analysis: Data are presented as means ± SD. Continuous variables were compared among groups using One-way analysis of variance (ANOVA) and post hoc

comparisons were made using Tukey's test, while comparisons concerning the ACh- and Gtn-relaxation and tension data were analyzed by Two-way analysis of variance (ANOVA) and Tukey's test. For the calculation of P values, no assumption of equal variability of differences was performed and data were corrected with Geisser-Greenhouse correction. A value of $P<0.05$ was considered statistically significant (*$P<0.05$, **$P<0.01$, ***$P<0.005$ and ****$P<0.001$). All statistical analyses and graph preparation were performed using GraphPad Prism 8 5 analysis software (GraphPad Software, Inc., La Jolla, CA). No outliers due to biological diversity were excluded. Samples that did not meet our technical criteria (i.e., poor staining, low mRNA or protein content) were not included into the analyses *a priori*. The confirmation of the absence of outlying values was confirmed by GraphPad Prism analysis software, using ROUT method and Q=1%. Complete statistical analysis is included in an additional supplemental file.

Supplementary References

1. Panova-Noeva M, Schulz A, Hermanns MI, Grossmann V, Pefani E, Spronk HM, Laubert-Reh D, Binder H, Beutel M, Pfeiffer N, Blankenberg S, Zeller T, Munzel T, Lackner KJ, Ten Cate H, Wild PS. Sex-specific differences in genetic and nongenetic determinants of mean platelet volume: results from the Gutenberg Health Study. Blood 2016;**127**(2):251-9.
2. Coleman JL, Brennan K, Ngo T, Balaji P, Graham RM, Smith NJ. Rapid Knockout and Reporter Mouse Line Generation and Breeding Colony Establishment Using EUCOMM Conditional-Ready Embryonic Stem Cells: A Case Study. Front Endocrinol (Lausanne) 2015;**6**:105.
3. Skarnes WC, Rosen B, West AP, Koutsourakis M, Bushell W, Iyer V, Mujica AO, Thomas M, Harrow J, Cox T, Jackson D, Severin J, Biggs P, Fu J, Nefedov M, de Jong PJ, Stewart AF, Bradley A. A conditional knockout resource for the genome-wide study of mouse gene function. Nature 2011;**474**(7351):337-42.
4. Liput DJ. Cre-Recombinase Dependent Germline Deletion of a Conditional Allele in the Rgs9cre Mouse Line. Front Neural Circuits 2018;**12**:68.
5. Clausen BE, Burkhardt C, Reith W, Renkawitz R, Forster I. Conditional gene targeting in macrophages and granulocytes using LysMcre mice. Transgenic Res 1999;**8**(4):265-77.
6. Forde A, Constien R, Grone HJ, Hammerling G, Arnold B. Temporal Cre-mediated recombination exclusively in endothelial cells using Tie2 regulatory elements. Genesis 2002;**33**(4):191-7.
7. Wirth A, Benyo Z, Lukasova M, Leutgeb B, Wettschureck N, Gorbey S, Orsy P, Horvath B, Maser-Gluth C, Greiner E, Lemmer B, Schutz G, Gutkind JS, Offermanns S. G12-G13-LARG-mediated signaling in vascular smooth muscle is required for salt-induced hypertension. Nat Med 2008;**14**(1):64-8.
8. Kilkenny C, Browne W, Cuthill IC, Emerson M, Altman DG, National Centre for the Replacement R, Reduction of Amimals in R. Animal research: reporting in vivo experiments--the ARRIVE guidelines. J Cereb Blood Flow Metab 2011;**31**(4):991-3.
9. Kossmann S, Lagrange J, Jackel S, Jurk K, Ehlken M, Schonfelder T, Weihert Y, Knorr M, Brandt M, Xia N, Li H, Daiber A, Oelze M, Reinhardt C, Lackner K, Gruber A, Monia B, Karbach SH, Walter U, Ruggeri ZM, Renne T, Ruf W, Munzel T, Wenzel P. Platelet-localized FXI promotes a vascular coagulation-inflammatory circuit in arterial hypertension. Sci Transl Med 2017;**9**(375).
10. Molitor M, Rudi WS, Garlapati V, Finger S, Schuler R, Kossmann S, Lagrange J, Nguyen TS, Wild J, Knopp T, Karbach SH, Knorr M, Ruf W, Munzel T, Wenzel P. Nox2+ Myeloid cells drive vascular inflammation and endothelial dysfunction in heart failure after myocardial infarction via angiotensin II receptor type 1. Cardiovasc Res 2020.

11. Lockette WE, Webb RC, Bohr DF. Prostaglandins and potassium relaxation in vascular smooth muscle of the rat. The role of Na-K ATPase. Circ Res 1980;**46**(5):714-20.
12. Sawada H, Chen JZ, Wright BC, Moorleghen JJ, Lu HS, Daugherty A. Ultrasound Imaging of the Thoracic and Abdominal Aorta in Mice to Determine Aneurysm Dimensions. J Vis Exp 2019(145).
13. Brandt M, Giokoglu E, Garlapati V, Bochenek ML, Molitor M, Hobohm L, Schonfelder T, Munzel T, Kossmann S, Karbach SH, Schafer K, Wenzel P. Pulmonary Arterial Hypertension and Endothelial Dysfunction Is Linked to NADPH Oxidase-Derived Superoxide Formation in Venous Thrombosis and Pulmonary Embolism in Mice. Oxid Med Cell Longev 2018;**2018**:1860513.
14. Wheeler JB, Mukherjee R, Stroud RE, Jones JA, Ikonomidis JS. Relation of murine thoracic aortic structural and cellular changes with aging to passive and active mechanical properties. J Am Heart Assoc 2015;**4**(3):e001744.
15. Bhatta A, Yao L, Toque HA, Shatanawi A, Xu Z, Caldwell RB, Caldwell RW. Angiotensin II-induced arterial thickening, fibrosis and stiffening involves elevated arginase function. PLoS One 2015;**10**(3):e0121727.
16. Bochenek ML, Leidinger C, Rosinus NS, Gogiraju R, Guth S, Hobohm L, Jurk K, Mayer E, Munzel T, Lankeit M, Bosmann M, Konstantinides S, Schafer K. Activated Endothelial TGFbeta1 Signaling Promotes Venous Thrombus Nonresolution in Mice Via Endothelin-1: Potential Role for Chronic Thromboembolic Pulmonary Hypertension. Circ Res 2020;**126**(2):162-181.
17. Adhikari N, Shekar KC, Staggs R, Win Z, Steucke K, Lin YW, Wei LN, Alford P, Hall JL, International Society of Cardiovascular Translational R. Guidelines for the isolation and characterization of murine vascular smooth muscle cells. A report from the International Society of Cardiovascular Translational Research. J Cardiovasc Transl Res 2015;**8**(3):158-63.
18. Efentakis P, Varela A, Chavdoula E, Sigala F, Sanoudou D, Tenta R, Gioti K, Kostomitsopoulos N, Papapetropoulos A, Tasouli A, Farmakis D, Davos CH, Klinakis A, Suter T, Cokkinos DV, Iliodromitis EK, Wenzel P, Andreadou I. Levosimendan prevents doxorubicin-induced cardiotoxicity in time- and dose dependent manner: Implications for inotropy. Cardiovasc Res 2019.
19. Jonkman J, Brown CM, Wright GD, Anderson KI, North AJ. Guidance for quantitative confocal microscopy. Nat Protoc 2020.
20. Rani S, Sreenivasaiah PK, Kim JO, Lee MY, Kang WS, Kim YS, Ahn Y, Park WJ, Cho C, Kim DH. Tauroursodeoxycholic acid (TUDCA) attenuates pressure overload-induced cardiac remodeling by reducing endoplasmic reticulum stress. PLoS One 2017;**12**(4):e0176071.

21. Luo H, Zhou C, Chi J, Pan S, Lin H, Gao F, Ni T, Meng L, Zhang J, Jiang C, Ji Z, Lv H, Guo H. The Role of Tauroursodeoxycholic Acid on Dedifferentiation of Vascular Smooth Muscle Cells by Modulation of Endoplasmic Reticulum Stress and as an Oral Drug Inhibiting In-Stent Restenosis. Cardiovasc Drugs Ther 2019;**33**(1):25-33.

Supplemental Figure Legends

Figure S1: Population Studies demonstrating TBCE single nucleotide polymorphisms. Identification of TBCE SNP **A.** rs6675944 and **B.** rs12405889 in population studies originating from worldwide databases. (Databases: Trans-Omics for Precision Medicine (TOPMed) Program, NHLBI established WGS project; Genome Aggregation Database (gnomAD); 1000 Genomes Project, International Genome Sample Resource (IGSR); Tasa T et al. Eur J Human Genet. 27; 442–454, 2019; The Avon Longitudinal Study of Parents and Children project, Bristol UK; UK10K Rare Genetic Variants in Health and Disease project, Sanger Institute; https://gtexportal.org.).

Figure S2: **Generation of the conditional TBCE knockdown mice. A.** Diagram of breeding technique for generating the transgenic mice **B.** Table of PCR primers used for genotyping. Representative PCR gel images for generation of **C.** Tm1c mice **D.** LysMCre$^{+/-}$TBCE^{tm2c} mice **E.** Tie2-ERT2-Cre$^{+/-}$TBCE^{tm2c} **F.** SMMHC-ERT2-Cre$^{+/-}$TBCE^{tm2c}; according to EUCOMM terminology, tm2c symbolizes the transgenic mice with the floxed gene (e.g., TBCE$^{fl/fl}$ were homozygous TBCE^{tm2c}). **G**. Workflow of the interventions performed on the conditional knockout mice.

Figure S3: Survival rates and biometric analyses of the conditional TBCE knockdown mice. Kaplan-Meier curves of **A.** LysMCre$^{+/-}$TBCE$^{fl/fl}$**, B.** Tie2-ERT2-Cre$^{+/-}$TBCE$^{fl/fl}$ and **C.** SMMHC-ERT2-Cre$^{+/-}$TBCE$^{fl/fl}$ mice. **D.** Table of body weight (g), postprandial blood glucose (mg/dl), triglycerides (mg/dl) and total cholesterol (mg/dl) of the TBCE knockdown and C57bl/6J background control mice (n=6 per group; Tukey's multiple comparison test; One-way ANOVA of variances).

Figure S4: TBCE knockdown in myeloid cells results in no significant vascular phenotype in the LysMCre$^{+/-}$TBCE$^{fl/fl}$ mice. Representative graphs of **A.** (%) Relaxation and **B.** Tension (g) curves to ACh **C.** Maximal Contraction (g) to prostaglandin F2 α (PGF2α). **D.** (%) Relaxation and **E.** Tension (g) curves to GTN. Two-Way ANOVA, Tukey's multiple comparison test). **F.** Systolic blood pressure (mmHg) (n=6-9 per group). **G.** Sirius red (collagen) and Hematoxylin-Eosin staining of murine aortas and graphs of **H.** Media thickness (n=4 per group) and **L.** Collagen/Media thickness (μm) (n=4 per group); bars represent 20μm and images were gained at a 40x magnification (Tukey's multiple comparison test; One-way ANOVA of variances).

Figure S5: TBCE regulation in renal microcirculation of Tie2-ERT2-Cre$^{+/-}$TBCE$^{fl/fl}$. Representative confocal images of renal microcirculation (glomeruli) and Integrated

fluorescence density graphs of TBCE/DAPI (normalized to ERT2-Cre$^{+/-}$TBCE$^{wt/wt}$) of kidney samples of the Tie2-ERT2-Cre$^{+/-}$TBCE$^{fl/fl}$. n=3 per group; Unpaired two-way Student's T-test; red:α-smooth muscle actin (α-SMA), green: TBCE, blue: DAPI and merged images of the channels; 40x magnification, white bar corresponds to 40µm.

Figure S6: Tie2-ERT2-Cre$^{+/-}$TBCE$^{fl/fl}$ mice have an endothelial specific TBCE ablation in the aortas. Representative immunofluorescence staining of Tie2-ERT2-Cre$^{+/-}$TBCE$^{fl/fl}$ aortas stained for DAPI (blue), TBCE (white) α-tubulin (red) (64x magnification, white bar represents 20 µm).

Figure S7: Endothelial TBCE deficiency leads to mildly increased vascular stiffness, and aortic wall thickening in response to AngII. (A-G) Concentration-contraction/relaxation curves of isolated aortic rings. **A.** Maximal Contraction (g) in response to prostaglandin F2 alpha (PGF2α). **B.** Vascular tension (g) curves in response to acetylcholine (ACh) or **C.** glycerol trinatrate (GTN) (Two-way ANOVA, Tukey's multiple comparison test). Vascular concentration-relaxation curves in response to ACh (**D** and **F**) and GTN of sham-operated (**D** and **F**) and AngII infused (1 mg/kg/day; **E** and **G**) mice (n=6-8 per group). **H.** Representative ultrasound images of B-Mode, M-Mode and PW Doppler of murine aortas and graphs of left common carotid artery (LCCA) **I.** Resistance index and **J.** Pulsatility index (n=5-6 per group). **K.** Sirius red (collagen) and hematoxylin-eosin staining of murine aortas and graphs showing the **L.** Media thickness (µm) (n=5-6 per group) and **M.**Collagen/Media thickness (n=4-6 per group) and; bars represent 20 µm and images were gained at 40x magnification (One-way ANOVA; Tukey's multiple comparison test).

Figure S8: Inflammatory vascular response and induction of ER stress in Tie2-ERT2-Cre$^{+/-}$TBCE$^{fl/fl}$ mice. A. RT-PCR data of mRNA expression of differentially regulated genes in the murine aortas (n=6 per group). Immunofluorescence images of **B.** murine aortas of AngII and sham infused Tie2-ERT2-Cre+/-TBCEfl/fl versus control mice and **C.** isolated pulmonary endothelial cells of sham infused Tie2-ERT2-Cre+/-TBCEfl/fl versus control mice (MPECs) with CD31 (red; endothelial marker), NLRP3 (green; inflammasome marker) and DAPI (blue; nuclear marker). Protein expression analysis of inflammasome and ER stress markers [protein kinase R (PKR)-like endoplasmic reticulum kinase (PERK); CCAAT/-enhancer-binding protein homologous protein (CHOP)] in murine primary endothelial cells (**D,** n=3 per group) and murine aortas (**E**, n=4-7 per group). Top: representative Western blot images; Bottom: Relative densitometry analysis. One-way ANOVA, Tukey's multiple comparison test).

Figure S9: Tie2-ERT2Cre$^{+/-}$TBCE$^{fl/fl}$ mice have a slightly augmented hypertensive phenotype in response AngII treatment. Graphs of **A.** Systolic and Diastolic blood pressure (n=7-8 per group). **B.** Representative M-Mode echocardiography images and **C.** Graphs of echocardiographic parameters LV mass (mg), SAX, M-Mode; Heart Rate (bpm); LV-EF (%), B-Mode; SV (µl) PLAX, M-Mode; LV PW sys (mm) PLAX, M-Mode; LV PW dia (mm) PLAX, M-Mode of Tie2-ERT2Cre$^{+/-}$TBCE$^{wt/wt}$ and Tie2-ERT2Cre$^{+/-}$TBCE$^{fl/fl}$ mice treated with AngII (n=5-6 per group; AngII 1 mg/kg/day). (Tukey's multiple comparison test; One-way ANOVA of variances). *LV, left ventricle; SAX, Short-axis view; bpm, beats per minute; EF, Ejection fraction; SV, Stroke volume; PW, posterior wall; sys, systole; PLAX, Parasternal Long Axis; dia, diastole.*

Figure S10: Endothelial specific TBCE knockout does not lead to significant aortic immune cell infiltration in Tie2-ERT2Cre$^{+/-}$TBCE$^{fl/fl}$ mice. (A-B) Flow cytometric analysis of isolated aortas from Tie2-ERT2Cre$^{+/-}$TBCE$^{fl/fl}$ and Tie2-ERT2Cre$^{+/-}$TBCE$^{wt/wt}$ control mice. **A.** Representative gating strategy of the Tie2-ERT2Cre$^{+/-}$TBCE$^{fl/fl}$ aortas **B.** Quantification of cell populations from analyzed aortas. Cell number per cm aorta is shown, n = 7–9 mice per group. **C.** Representative plots of flow cytometric analysis. CD11b^{+} cells (upper panel) were gated on living, CD45^{+} cells and Ly6G^{+}Ly6C^{+} neutrophils and Ly6C^{+}Ly6G^{-} monocytic cells (lower panel) were gated on living, CD45^{+}CD11b^{+} cells.

Figure S11: TBCE regulation in renal microcirculation and aortas of SMMHC-ERT2-Cre$^{+/-}$TBCE$^{fl/fl}$ mice. (A-B) Representative confocal images of renal microcirculation (glomeruli) and Integrated fluorescence density graphs of TBCE/DAPI (normalized to ERT2-Cre$^{+/-}$TBCE$^{wt/wt}$) of kidney samples of the SMMHC-ERT2-Cre$^{+/-}$TBCE$^{fl/fl}$. n=3 per group; Unpaired two-way Student's T-test; red:α-smooth muscle actin (α-SMA), green: TBCE, blue: DAPI and merged images of the channels; 40x magnification, white bar corresponds to 40µm. **C.** Representative immunofluorescence staining of SMMHC-ERT2-Cre$^{+/-}$TBCE$^{fl/fl}$ aortas stained for DAPI (blue), TBCE (white) α-tubulin (red) (64x magnification, white bar represents 20 µm).

Figure S12: TBCE deficiency does not affect aortic diameter at baseline but aggravates carotid wall thickness in response to AngII treatment in the SMMHC-ERT2-Cre$^{+/-}$TBCE$^{fl/fl}$ mice. A. Representative ultrasound images of the aortic arch (B-Mode, upper panel) and Left Common Carotid Artery (M-Mode, lower panel) of the sham- and AngII-treated SMMHC-ERT2-Cre$^{+/-}$TBCE$^{fl/fl}$ mice. Graphs of **B.** Ascending (Asc), **C.** Transverse (trans) aorta diameter (mm) and **D.** Left Common Carotid Artery (LCCA) wall thickness (mm) (n=4-6 per group; Tukey's multiple comparison test; One-way ANOVA of variances).

Figure S13: AngII leads to a hypertensive phenotype in both SMMHC-ERT2Cre$^{+/-}$TBCE$^{wt/wt}$ and SMMHC-ERT2Cre$^{+/-}$TBCE$^{fl/fl}$ mice independently of TBCE ablation, while AngII induced a mild cardiac dysfunction only in the SMMHC-ERT2Cre$^{+/-}$TBCE$^{fl/fl}$ mice. Graphs of **A.** Systolic and Diastolic blood pressure (n=5-6 per group). **B.** Representative M-Mode echocardiography images and **C.** Graphs of echocardiographic parameters LV mass (mg), SAX, M-Mode; Heart Rate (bpm); LV-EF (%), B-Mode; SV (µl) PLAX, M-Mode; LV PW sys (mm) PLAX, M-Mode; LV PW dia (mm) PLAX, M-Mode of SMMHC-ERT2Cre$^{+/-}$TBCE$^{wt/wt}$ and SMMHC-ERT2Cre$^{+/-}$TBCE$^{fl/fl}$ mice treated with AngII (n=5-6 per group; AngII 1 mg/kg/day). (Tukey's multiple comparison test; 1way ANOVA of variances). *LV, left ventricle; SAX, Short-axis view; bpm, beats per minute; EF, Ejection fraction; SV, Stroke volume; PW, posterior wall; sys, systole; PLAX, Parasternal Long Axis; dia, diastole.*

Figure S14: VSMCs-specific TBCE knockout does not lead to significant immune cell infiltration in the aortas of the SMMHC-ERT2Cre$^{+/-}$TBCE$^{fl/fl}$ mice. (A-B) Flow cytometric analysis of isolated aortas from SMMHC-ERT2Cre$^{+/-}$TBCE$^{fl/fl}$ and SMMHC-ERT2Cre$^{+/-}$TBCE$^{wt/wt}$ control mice. **A.** Representative gating strategy of the SMMHC-ERT2Cre$^{+/-}$TBCE$^{fl/fl}$ aortas **B.** Quantification of cell populations from analyzed aortas. Cell number per cm aorta is shown, n = 5–10 mice per group. **C.** Representative plots of flow cytometric analysis. CD11b^{+} cells (upper panel) were gated on living, CD45^{+} cells and Ly6G^{+}Ly6C^{+} neutrophils and Ly6C^{+}Ly6G^{-} monocytic cells (lower panel) were gated on living, CD45^{+}CD11b^{+} cells.

Supplemental Figures

Figure S1

A

rs6675944

Study	Population	Group	Sample Size	Ref Allele	Alt Allele
TopMed	Global	Study-wide	125568	T=0.51001	C=0.48999
gnomAD - Genomes	Global	Study-wide	30852	T=0.5034	C=0.4966
gnomAD - Genomes	European	Sub	18442	T=0.4811	C=0.5189
gnomAD - Genomes	African	Sub	8692	T=0.591	C=0.409
gnomAD - Genomes	East Asian	Sub	1608	T=0.326	C=0.674
gnomAD - Genomes	Other	Sub	974	T=0.48	C=0.52
gnomAD - Genomes	American	Sub	834	T=0.47	C=0.53
gnomAD - Genomes	Ashkenazi Jewish	Sub	302	T=0.47	C=0.53
1000Genomes	Global	Study-wide	5008	T=0.499	C=0.501
1000Genomes	African	Sub	1322	T=0.597	C=0.403
1000Genomes	East Asian	Sub	1008	T=0.346	C=0.654
1000Genomes	Europe	Sub	1006	T=0.492	C=0.508
1000Genomes	South Asian	Sub	978	T=0.55	C=0.45
1000Genomes	American	Sub	694	T=0.48	C=0.52
Genetic variation in the Estonian population	Estonian	Study-wide	4480	T=0.450	C=0.550
The Avon Longitudinal Study of Parents and Children	Parent and Child Cohort	Study-wide	3854	T=0.516	C=0.484
UK 10K study - Twins	Twin Cohort	Study-wide	3708	T=0.495	C=0.505

B

rs12405889

Study	Population	Group	Sample Size	Ref Allele	Alt Allele
TopMed	Global	Study-wide	125568	T=0.48898	G=0.51102
gnomAD - Genomes	Global	Study-wide	30878	T=0.4882	G=0.5118
gnomAD - Genomes	European	Sub	18458	T=0.4673	G=0.5327
gnomAD - Genomes	African	Sub	8700	T=0.576	G=0.424
gnomAD - Genomes	East Asian	Sub	1604	T=0.323	G=0.677
gnomAD - Genomes	Other	Sub	978	T=0.47	G=0.53
gnomAD - Genomes	American	Sub	836	T=0.40	G=0.60
gnomAD - Genomes	Ashkenazi Jewish	Sub	302	T=0.44	G=0.56
1000Genomes	Global	Study-wide	5008	T=0.480	G=0.520
1000Genomes	African	Sub	1322	T=0.594	G=0.406
1000Genomes	East Asian	Sub	1008	T=0.343	G=0.657
1000Genomes	Europe	Sub	1006	T=0.481	G=0.519
1000Genomes	South Asian	Sub	978	T=0.51	G=0.49
1000Genomes	American	Sub	694	T=0.42	G=0.58
Genetic variation in the Estonian population	Estonian	Study-wide	4480	T=0.440	G=0.560
The Avon Longitudinal Study of Parents and Children	Parent and Child Cohort	Study-wide	3854	T=0.501	G=0.499
UK 10K study - Twins	Twin Cohort	Study-wide	3708	T=0.477	G=0.523

547 **Figure S2**

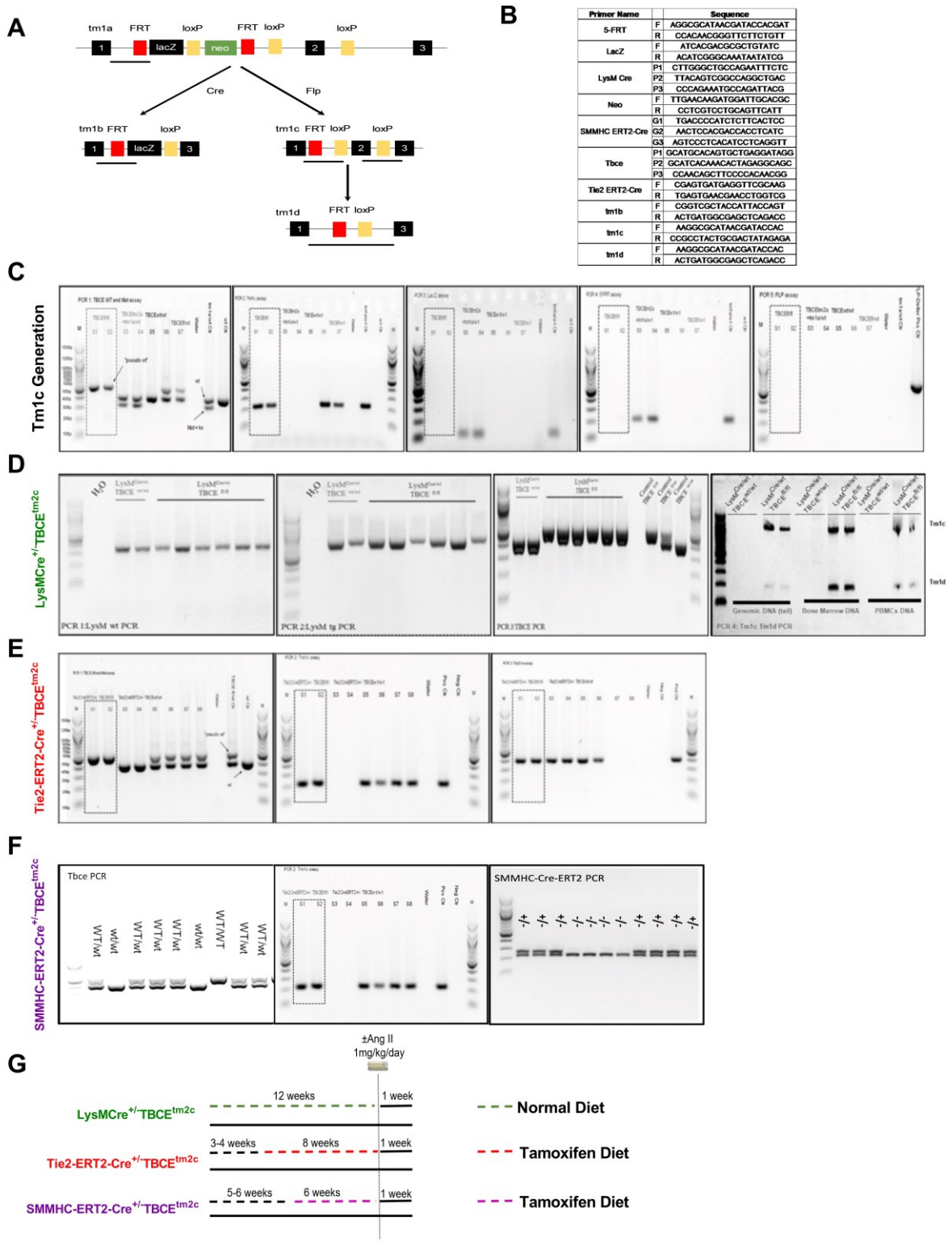

Primer Name		Sequence
5-FRT	F	AGGCGCATAACGATACCACGAT
	R	CCACAACGGGTTCTTCTGTT
LacZ	F	ATCACGACGCGCTGTATC
	R	ACATCGGGCAAATAATATCG
LysM Cre	P1	CTTGGGCTGCCAGAATTTCTC
	P2	TTACAGTCGGCCAGGCTGAC
	P3	CCCAGAAATGCCAGATTACG
Neo	F	TTGAACAAGATGGATTGCACGC
	R	CCTCGTCCTGCAGTTCATT
SMMHC ERT2-Cre	G1	TGACCCCATCTCTTCACTCC
	G2	AACTCCACGACCACCTCATC
	G3	AGTCCCTCACATCCTCAGGTT
Tbce	P1	GCATGCACAGTGCTGAGGATAGG
	P2	GCATCACAAACACTAGAGGCAGC
	P3	CCAACAGCTTCCCCACAACGG
Tie2 ERT2-Cre	F	CGAGTGATGAGGTTCGCAAG
	R	TGAGTGAACGAACCTGGTCG
tm1b	F	CGGTCGCTACCATTACCAGT
	R	ACTGATGGCGAGCTCAGACC
tm1c	F	AAGGCGCATAACGATACCAC
	R	CCGCCTACTGCGACTATAGAGA
tm1d	F	AAGGCGCATAACGATACCAC
	R	ACTGATGGCGAGCTCAGACC

548

549 **Figure S3**

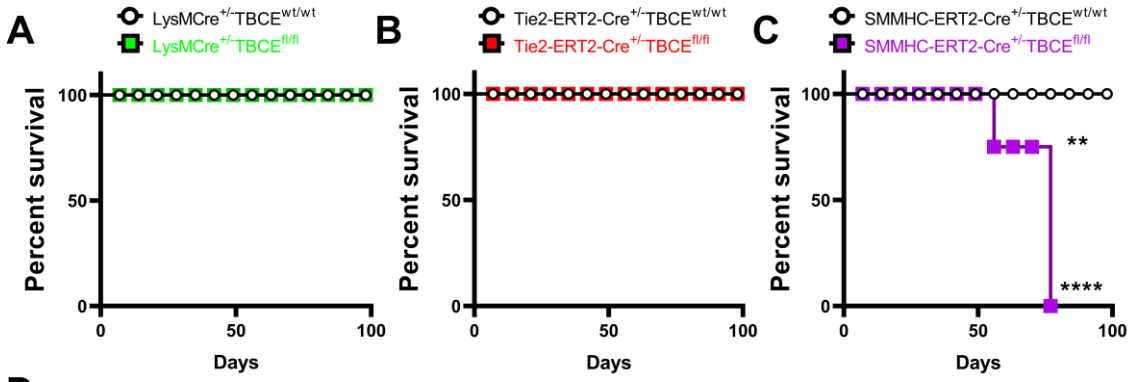

D

	C57BL/6J (n=6)	LysMCre$^{+/-}$ TBCE$^{wt/wt}$ (n=6)	LysMCre$^{+/-}$ TBCE$^{fl/fl}$ (n=6)	Tie2-ERT2-Cre$^{+/-}$ TBCE$^{wt/wt}$ (n=6)	Tie2-ERT2-Cre$^{+/-}$ TBCE$^{fl/fl}$ (n=6)	SMMHC-ERT2-Cre$^{+/-}$TBCE$^{wt/wt}$ (n=6)	SMMHC-ERT2-Cre$^{+/-}$TBCE$^{fl/fl}$ (n=6)
Body Weight (g)	24.12±0.5	26.17±0.79	25.5±0.92	21.26±0.23$^{\#\#}$	18.25±0.53$^{***\#\#\#}$	18.72±0.48$^{\#\#\#\#}$	19.49±0.54$^{\#\#\#}$
Blood Glucose (mg/dl)	149.4±3.8	110.0±3.9	122.0±22.5	149.6±13.2	130.6±7.9	128.8±12.6	126.2±4.9
Triglycerides (mg/dl)	77.0±10.3	67.6±6.5	82.4±12.87	72.4±10.7	67.8±10.0	102.4±14.8	82.6±10.0
Total Cholesterol (mg/dl)	57.2±1.8	59.6±4.2	57.0±2.4	37.8±5.7$^{\#}$	40.4±5.6$^{\#}$	40.8±4.9$^{\#\#}$	35.2±1.5$^{\#\#\#}$

550

551

552 **Figure S4**

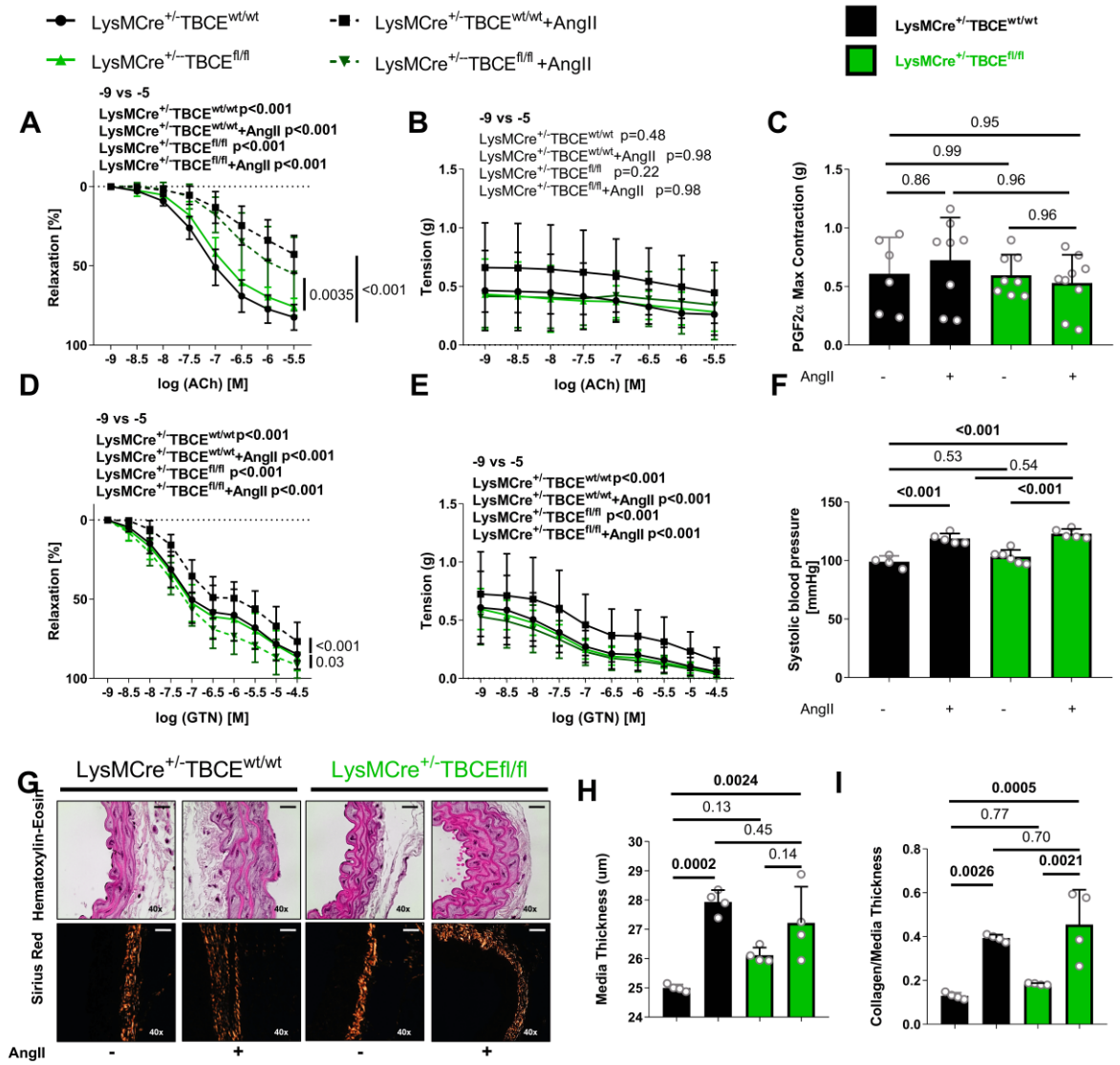

553

554

Figure S5

-

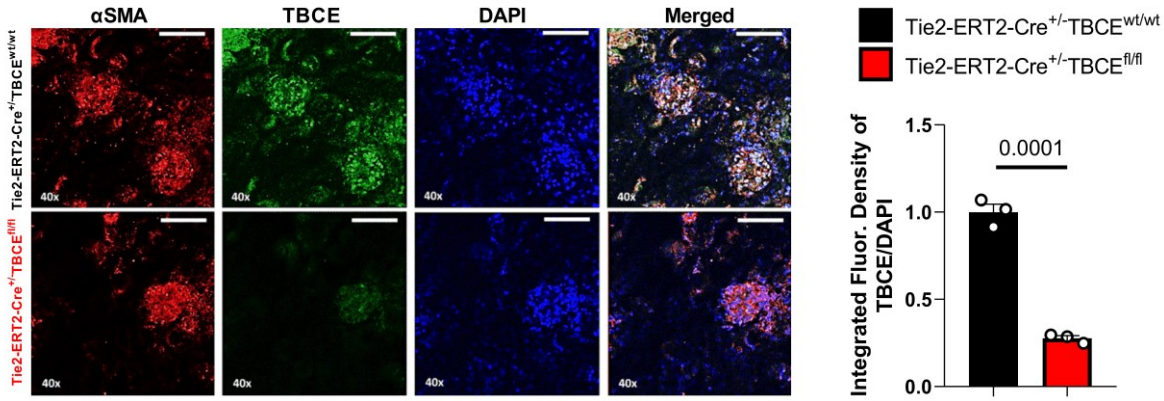
αSMA
TBCE
DAPI
Merged
Tie2-ERT2-Cre+/-TBCEwt/wt
Tie2-ERT2-Cre+/-TBCEfl/fl
40x
Tie2-ERT2-Cre+/-TBCEwt/wt
Tie2-ERT2-Cre+/-TBCEfl/fl
Integrated Fluor. Density of TBCE/DAPI
0.0001
1.5
1.0
0.5
0.0

Figure S6

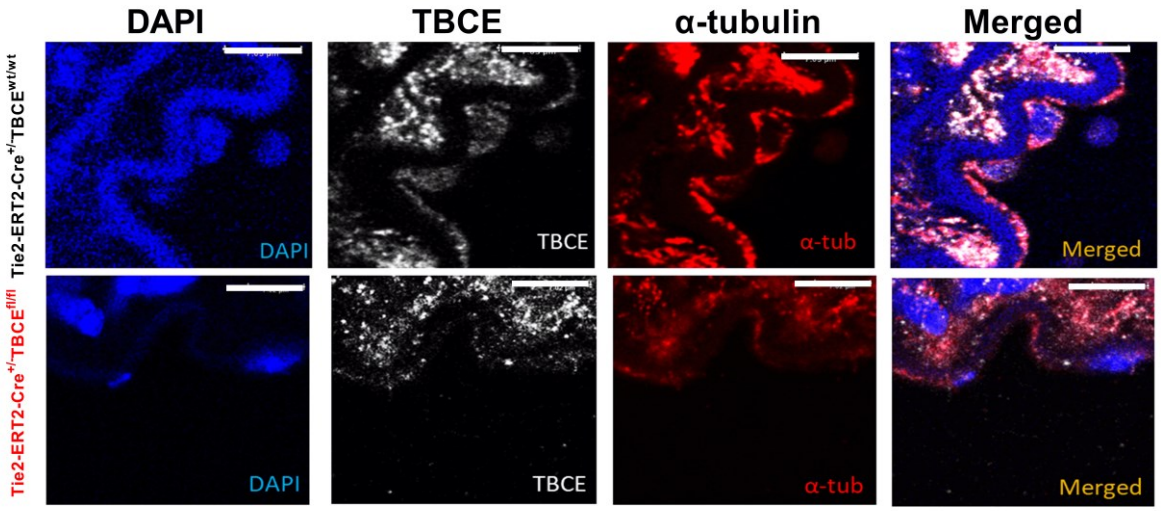
DAPI
TBCE
α-tubulin
Merged
Tie2-ERT2-Cre+/-TBCEwt/wt
Tie2-ERT2-Cre+/-TBCEfl/fl
DAPI
TBCE
α-tub
Merged
DAPI
TBCE
α-tub
Merged

561 **Figure S7**

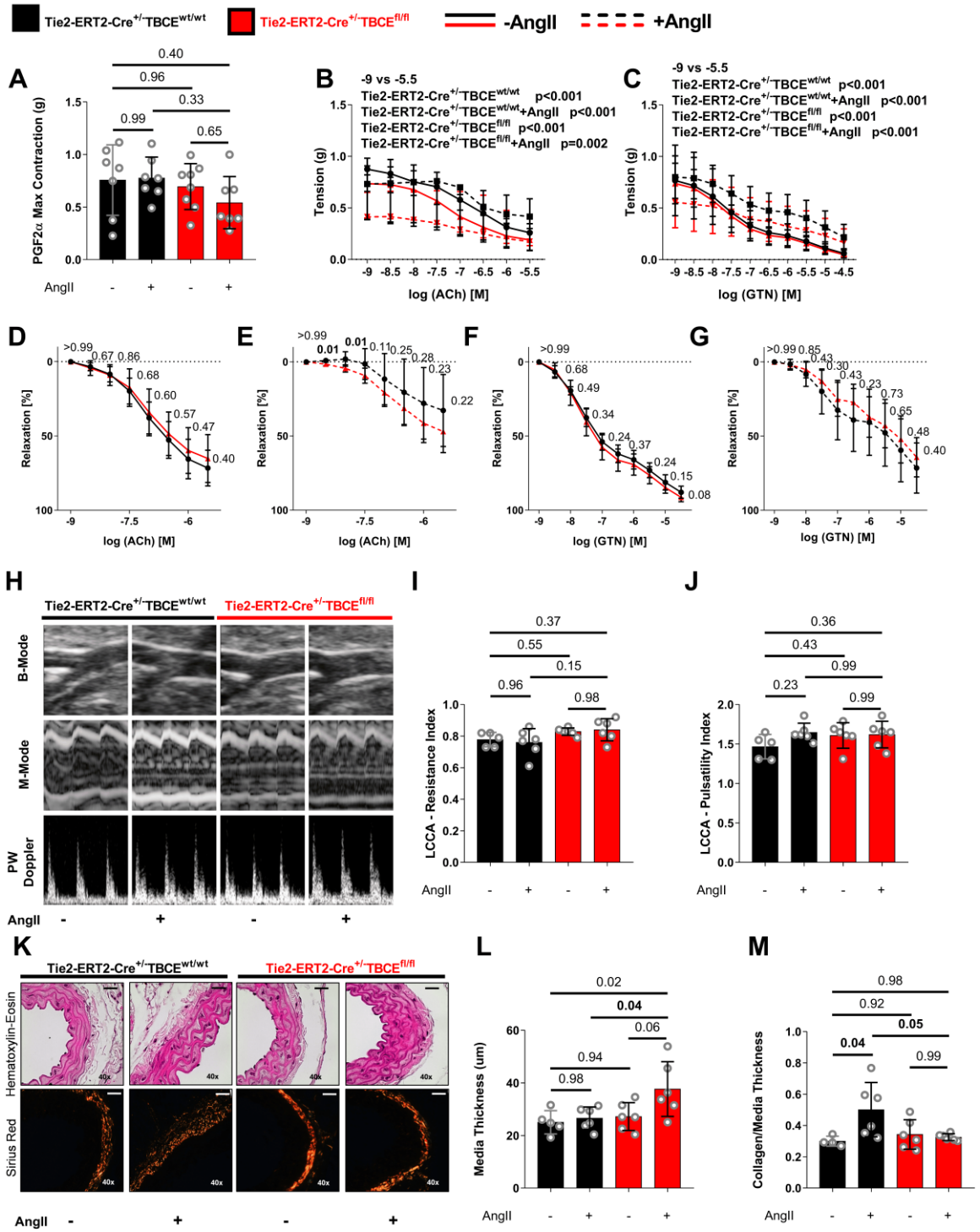

562

563

564 **Figure S8**

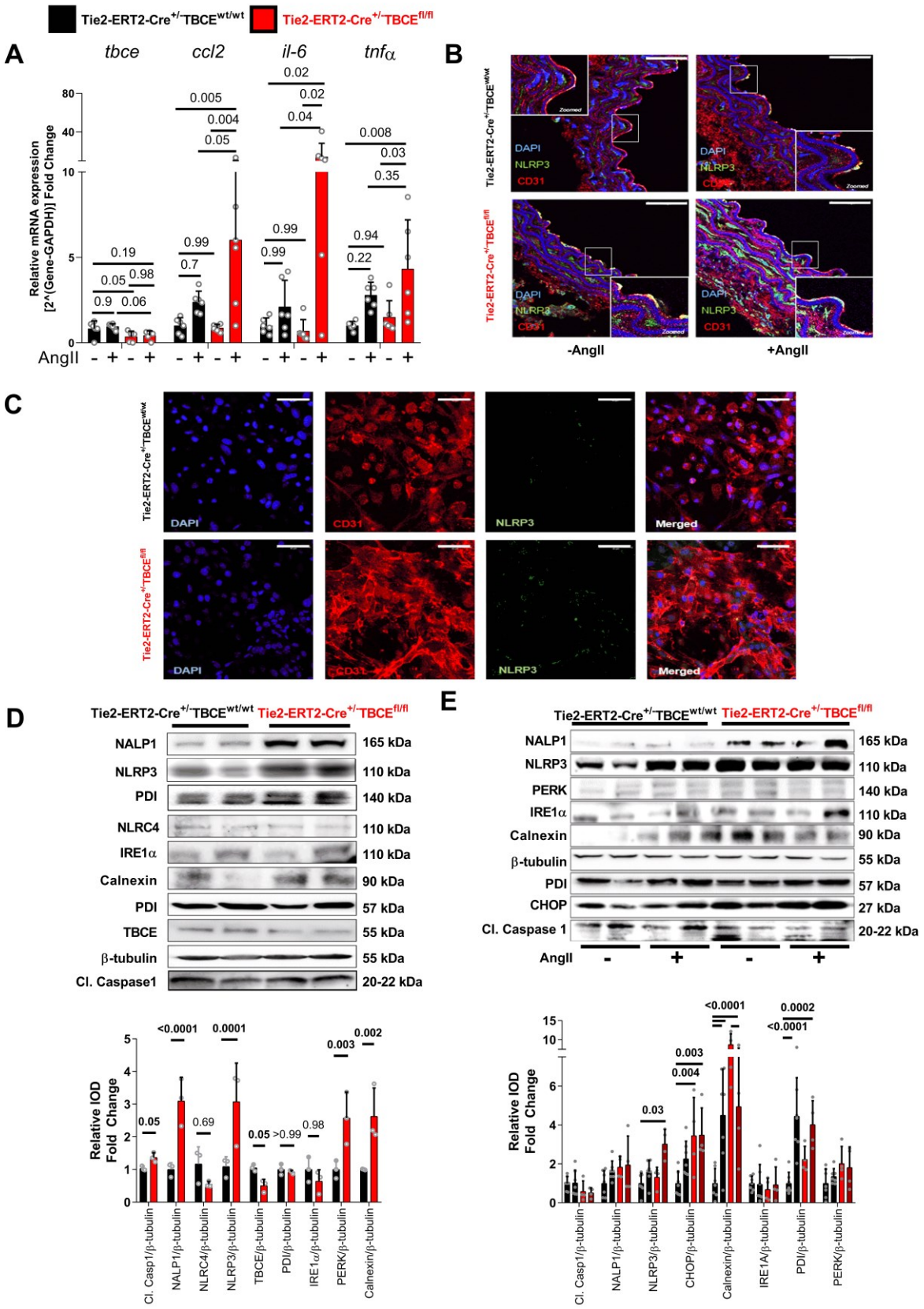

565

566

567

Figure S9

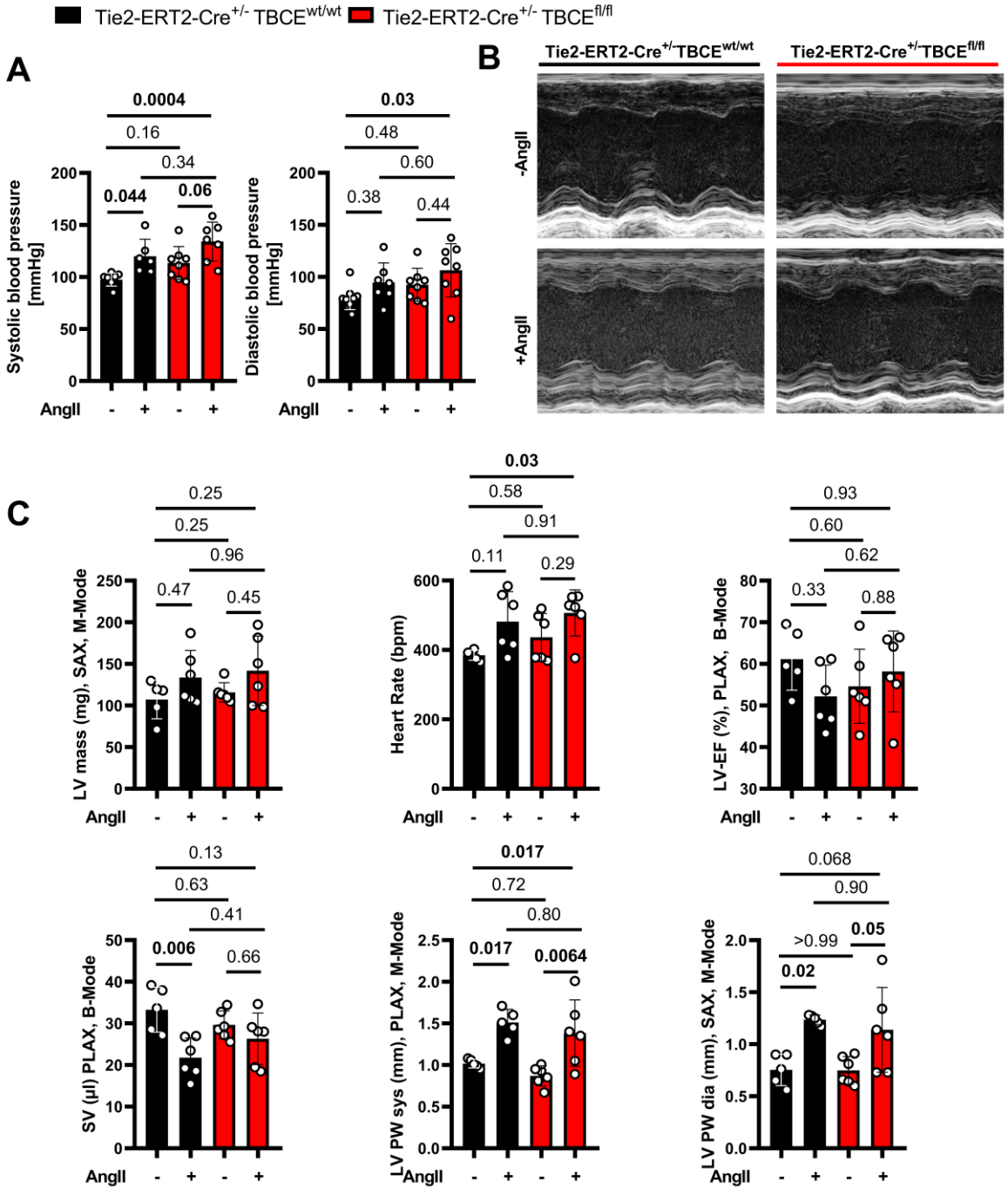
Tie2-ERT2-Cre+/- TBCEwt/wt
Tie2-ERT2-Cre+/- TBCEfl/fl
A
Systolic blood pressure [mmHg]
Diastolic blood pressure [mmHg]
AngII
B
Tie2-ERT2-Cre+/-TBCEwt/wt
Tie2-ERT2-Cre+/-TBCEfl/fl
-AngII
+AngII
C
LV mass (mg), SAX, M-Mode
Heart Rate (bpm)
LV-EF (%), PLAX, B-Mode
SV (µl) PLAX, B-Mode
LV PW sys (mm), PLAX, M-Mode
LV PW dia (mm), SAX, M-Mode

572 **Figure S10**

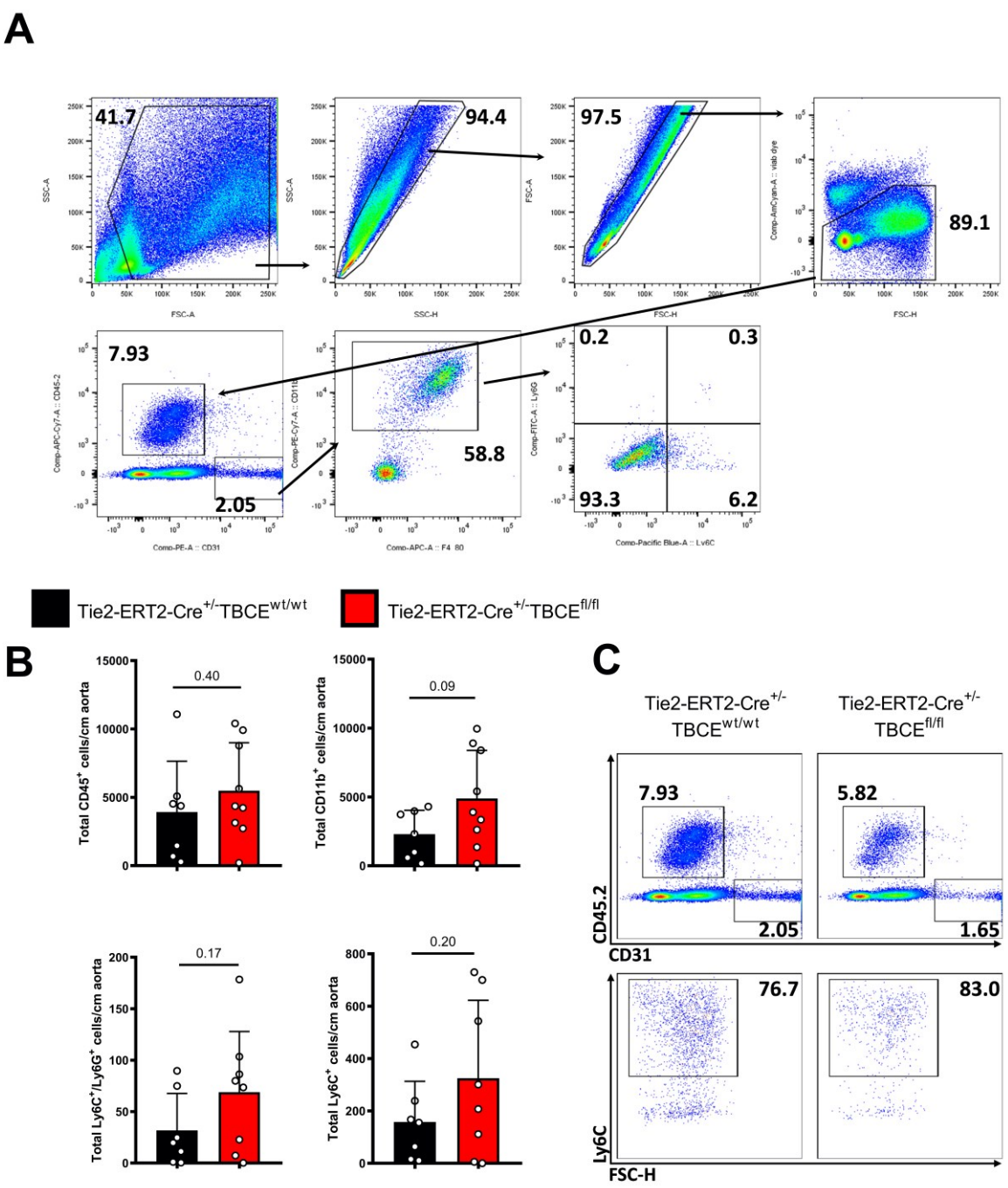

573

574

Figure S11

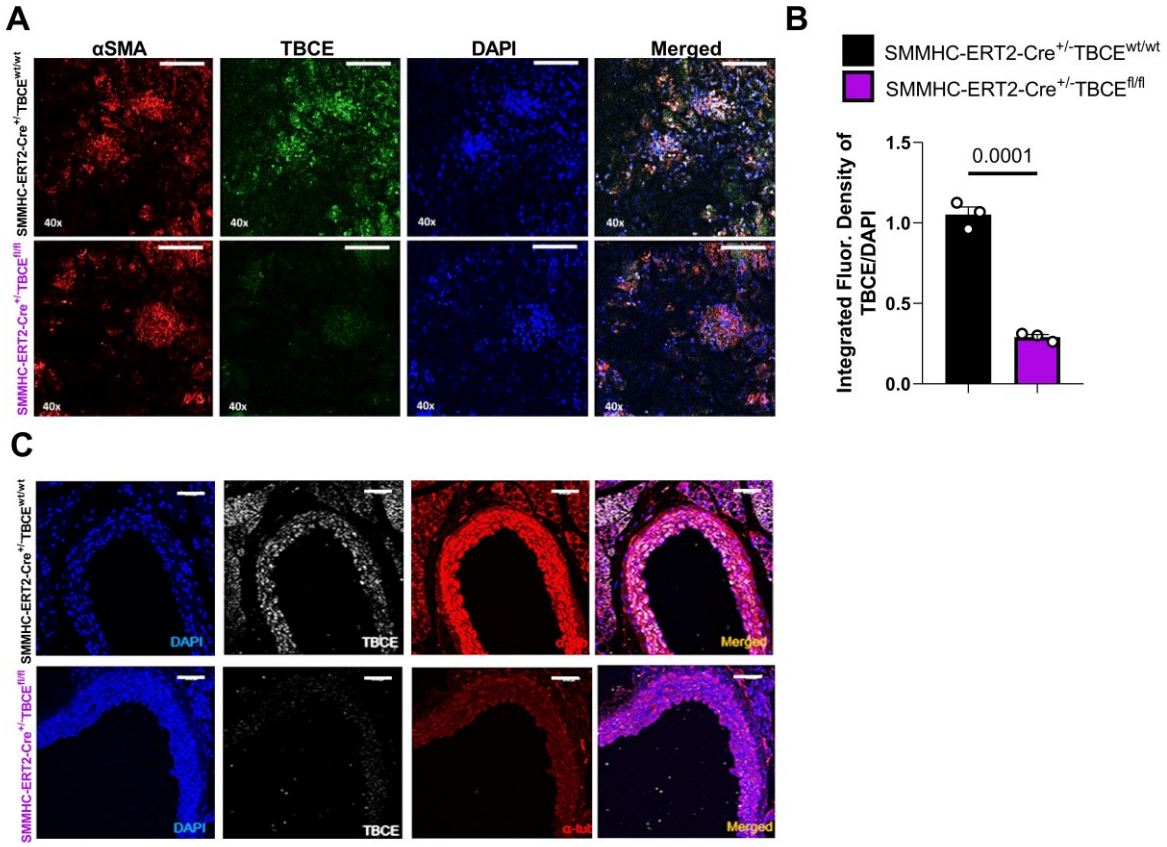
A
αSMA
TBCE
DAPI
Merged
SMMHC-ERT2-Cre+/-TBCEwt/wt
SMMHC-ERT2-Cre+/-TBCEfl/fl
40x
B
SMMHC-ERT2-Cre+/-TBCEwt/wt
SMMHC-ERT2-Cre+/-TBCEfl/fl
Integrated Fluor. Density of TBCE/DAPI
1.5
1.0
0.5
0.0
0.0001
C
SMMHC-ERT2-Cre+/-TBCEwt/wt
SMMHC-ERT2-Cre+/-TBCEfl/fl
DAPI
TBCE
α-tub
Merged

577 **Figure S12**

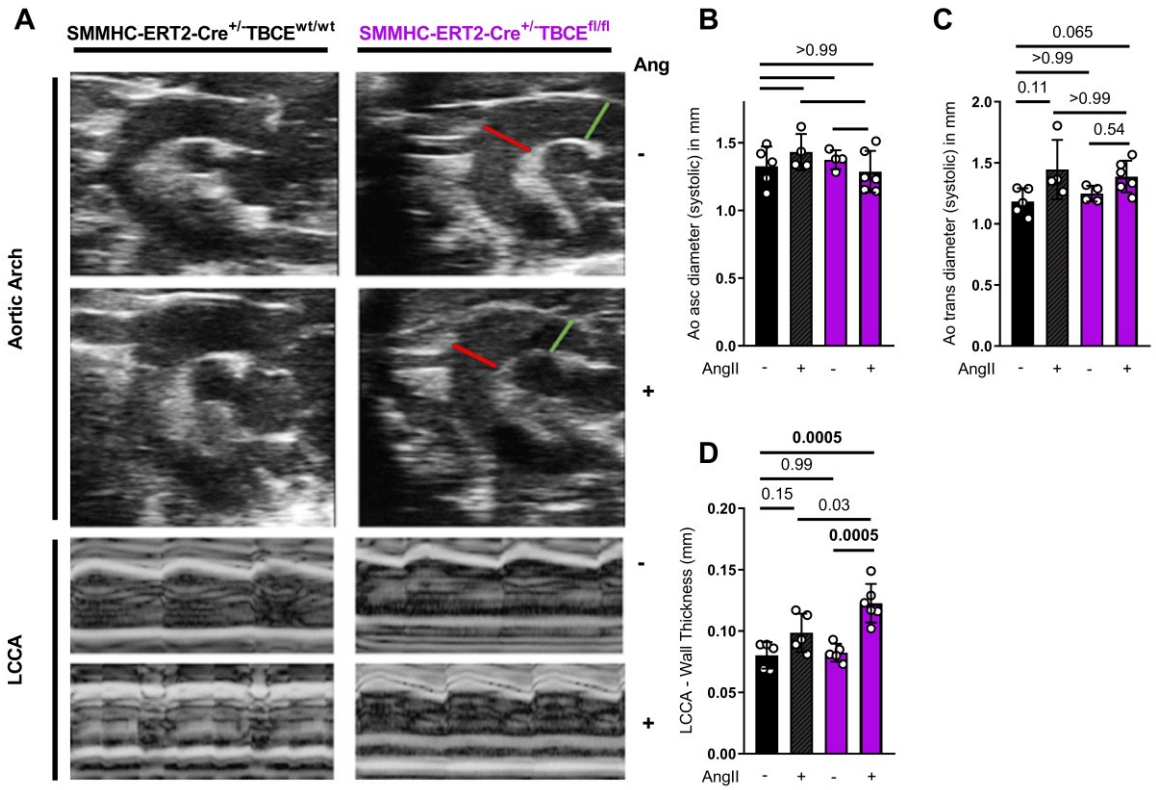

578

579

Figure S13

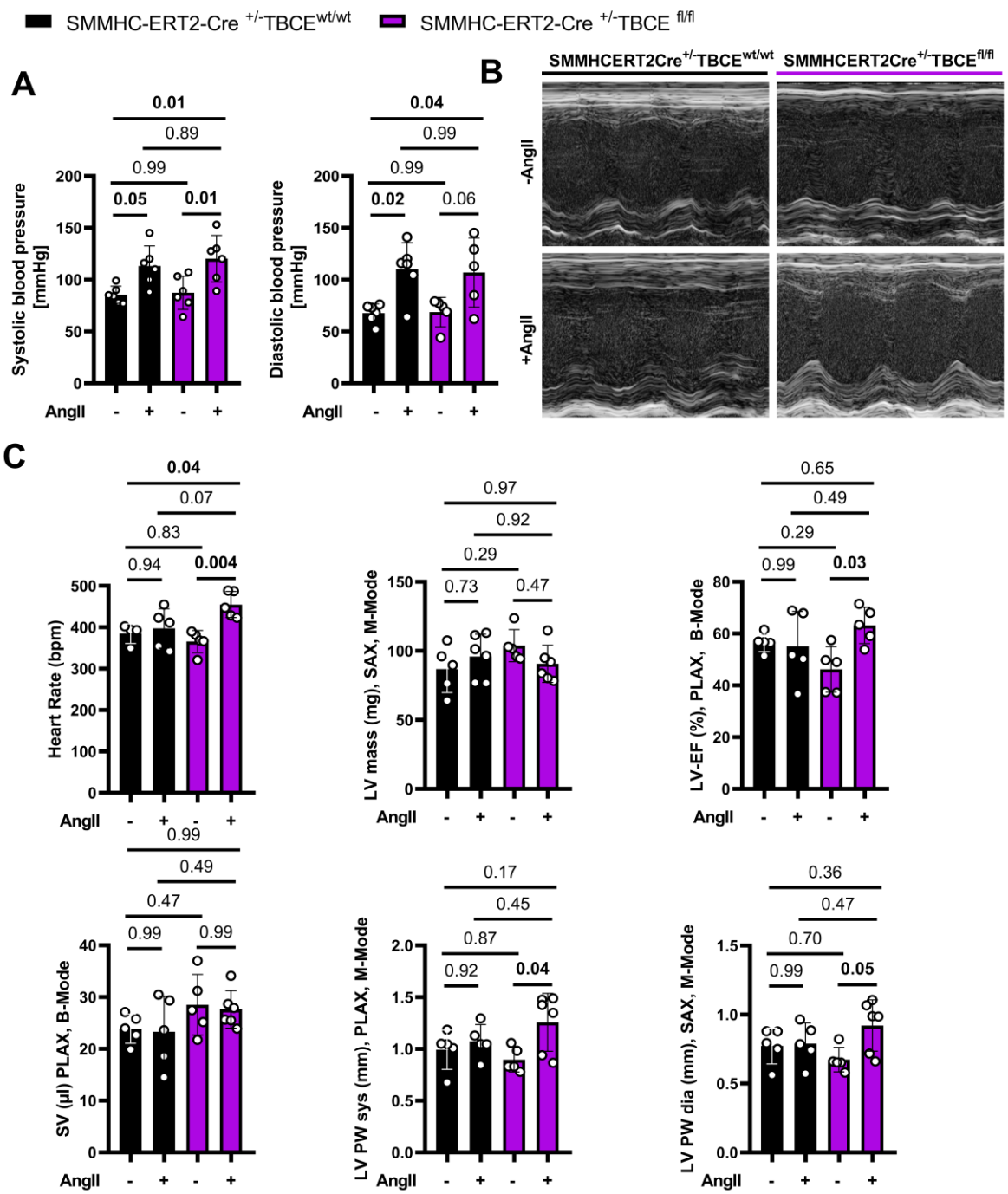
SMMHC-ERT2-Cre +/-TBCEwt/wt
SMMHC-ERT2-Cre +/-TBCE fl/fl
A
Systolic blood pressure [mmHg]
Diastolic blood pressure [mmHg]
AngII
B
SMMHCERT2Cre+/-TBCEwt/wt
SMMHCERT2Cre+/-TBCEfl/fl
-AngII
+AngII
C
Heart Rate (bpm)
LV mass (mg), SAX, M-Mode
LV-EF (%), PLAX, B-Mode
SV (µl) PLAX, B-Mode
LV PW sys (mm), PLAX, M-Mode
LV PW dia (mm), SAX, M-Mode

584 **Figure S14**

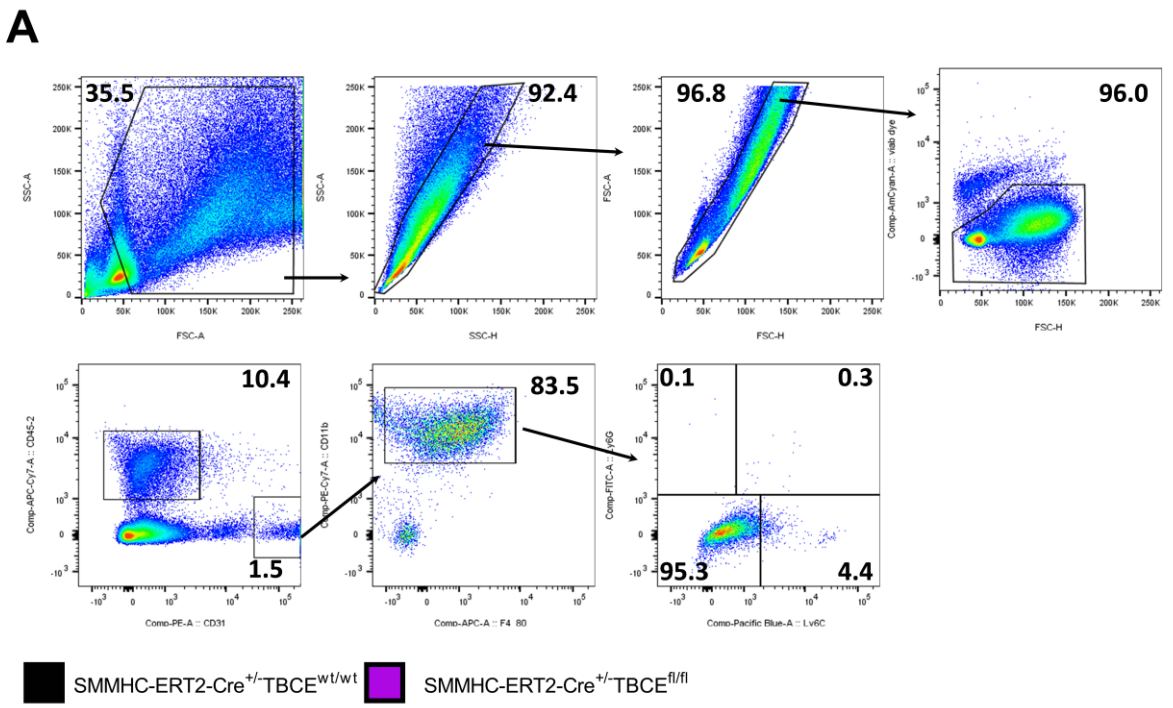

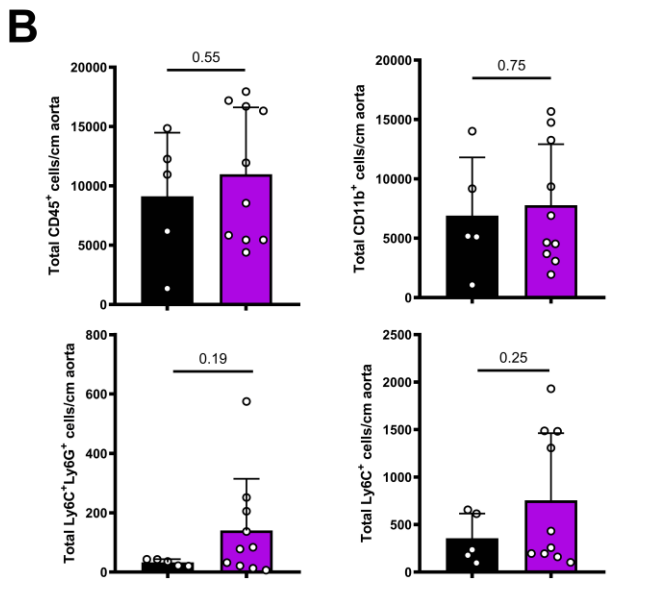

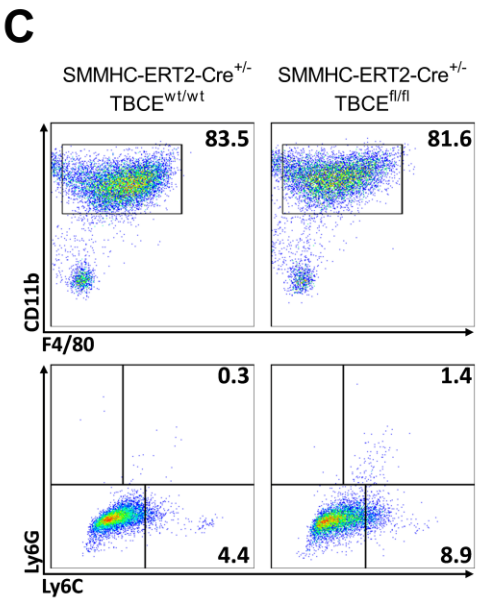

585

586

587